Supporting information

Density functional theory calculations of atomic, electronic and thermodynamic properties of cubic $LaCoO_3$ and $La_{1-x}Sr_xCoO_3$ surfaces

Shuguang Zhang,[*,†,‡] **Ning Han,**[†] **Xiaoyao Tan** [§]

[†] *School of Chemical Engineering, Shandong University of Technology, Zibo 255049, China*

[‡] *Department of Chemical and Biomolecular Engineering, University of Notre Dame, Notre Dame 46556, USA*

[§] *Department of Chemical Engineering, Tianjin Polytechnic University, Tianjin 300387, China*

[*] *Corresponding author. E-mail: gregzhangsg@gmail.com*

Table S1. Optimized lattice constants, local magnetic moment, Bader charges of 2×2×2 cubic $La_{0.875}Sr_{0.125}CoO_3$ structure.

$a = b = c$ (Å)		3.858
local magnetic moment (μ_B, per Co atom)		1.48-1.53 (1.77)
Spin state		LS/IS ($t_{2g}^{5+\delta}e_g^{1-\delta}$)
Bader charge (e, averaged over all ions of the same type)	q_{La}	2.094
	q_{Sr}	1.593
	q_{Co}	1.281
	q_O	-1.104

Table S2. Lattice parameters of metals and oxides involved in this study

Metal or oxide	Space group	Formula of unit cell	Calculated results	Experimental data[S1-S10]
Co	Fm-3m (225)	Co_4	$a = b = c = 3.549$ Å $\alpha = \beta = \gamma = 90^\circ$	$a = b = c = 3.544$ Å $\alpha = \beta = \gamma = 90^\circ$
La	P63/mmc (194)	La_4	$a = b = 3.759$ Å , $c = 12.117$ Å $\alpha = \beta = 90^\circ$, $\gamma = 120^\circ$	$a = b = 3.770$ Å , $c = 12.130$ Å $\alpha = \beta = 90^\circ$, $\gamma = 120^\circ$
Sr	Fm-3m (225)	Sr_4	$a = b = c = 6.040$ Å $\alpha = \beta = \gamma = 90^\circ$	$a = b = c = 6.085$ Å $\alpha = \beta = \gamma = 90^\circ$
Co_3O_4	Fd-3m (227)	$Co_{24}O_{32}$	$a = b = c = 8.144$ Å $\alpha = \beta = \gamma = 90^\circ$	$a = b = c = 8.082$ Å $\alpha = \beta = \gamma = 90^\circ$
CoO	Fm-3m (225)	Co_4O_4	$a = b = c = 4.253$ Å $\alpha = \beta = \gamma = 90^\circ$	$a = b = c = 4.263$ Å $\alpha = \beta = \gamma = 90^\circ$
La_2O_3	P-3m1 (164)	La_2O_3	$a = b = 3.948$ Å , $c = 6.183$ Å $\alpha = \beta = 90^\circ$, $\gamma = 120^\circ$	$a = b = 3.938$ Å , $c = 6.136$ Å $\alpha = \beta = 90^\circ$, $\gamma = 120^\circ$
SrO	Fm-3m (225)	Sr_4O_4	$a = b = c = 5.205$ Å $\alpha = \beta = \gamma = 90^\circ$	$a = b = c = 5.160$ Å $\alpha = \beta = \gamma = 90^\circ$
$SrCoO_3$	Pm-3m (221)	$SrCoO_3$	$a = b = c = 3.844$ Å $\alpha = \beta = \gamma = 90^\circ$	$a = b = c = 3.835$ Å $\alpha = \beta = \gamma = 90^\circ$
O_2	——	O_2	r (O-O): 1.23 Å v (O-O): 1563 cm^{-1}	r (O-O): 1.21 Å v (O-O): 1550 cm^{-1}

Table S3. Thermodynamics data for bulk La_2O_3, Co_3O_4, CoO, $LaCoO_3$, SrO and $SrCoO_3$. Calculated formation energies E^f and the experimental standard formation enthalpies (T^0 = 298.15 K, p^0 = 1 atm) are shown in the second and third columns, respectively. Data in the last column are obtained by extrapolating those in the third column to T = 0 K, p^0 = 1 atm.

Oxide	Calculated E^f (eV)	$\Delta H^{f,0}$ (eV)	ΔH^f (T = 0 K, eV)
La_2O_3	-17.32	-18.59[S11]	-18.61[S11]
Co_3O_4	-7.29	-9.23[S11]	-9.22[S11]
CoO	-1.68	-2.46[S11]	-2.49[S11]
$LaCoO_3$	-11.71	-12.77±0.06[S12]	-12.81[S13]±0.06[S12]
		-12.87±0.02[S14]	-12.91[S13]±0.06[S14]
		-13.04[S15]	-13.08[S15]
$LaCoO_3$ (from La_2O_3, CoO, O_2)	-1.37	-1.12±0.02[S14]	-1.11[S13]±0.02[S14]
SrO	-5.49	-6.14[S11]	-6.15
$SrCoO_3$	-8.57, this work; -9.80[S16], -7.01[S16], CALPHAD approach.		

Table S4. Parameters presented in the definition of the excess surface Gibbs free energy (Ω) for (001), (110) and (111) surfaces with different terminations.

Surface		$\Gamma^i_{La,O}$	$\Gamma^i_{La,Co}$	ϕ^i_{La} (eV/unit cell)	ϕ^i_{La} (J/m^2)
Orientation	Termination				
(001)	LaO	-4	-2	10.18	2.74
(001)	CoO_2	4	2	-2.12	-0.57
(110)	LaCoO	-4	0	12.21	2.33
(110)	O_2	4	0	5.28	1.01
(111)	LaO_3	0	-2	11.75	1.83
(111)	Co	0	2	5.53	0.86

Table S5. Calculated results of the correction term $\delta\mu_O^0$ for O atom chemical potential deviation.

Oxide	$\delta\mu_O^0$ (eV)
La_2O_3	0.11
Co_3O_4	0.17
CoO	0.46
SrO	0.33
Average	0.25 (undoped $LaCoO_3$) 0.27 (Sr-doped $LaCoO_3$)

Table S6. Calculated substitutional energies of Sr ions in different layers of the (001) surface slabs.

Energy	LaO-terminated (001) surface		CoO_2-terminated (001) surface	
(eV/ Sr ion)	1,7-doping	3,5-doping	2,6-doping	4-doping
$E_{Sr,substitutional}$	-0.88	-0.41	-0.38	-0.28
$\Delta E_{Sr,substitutional}$	0.47		0.10	

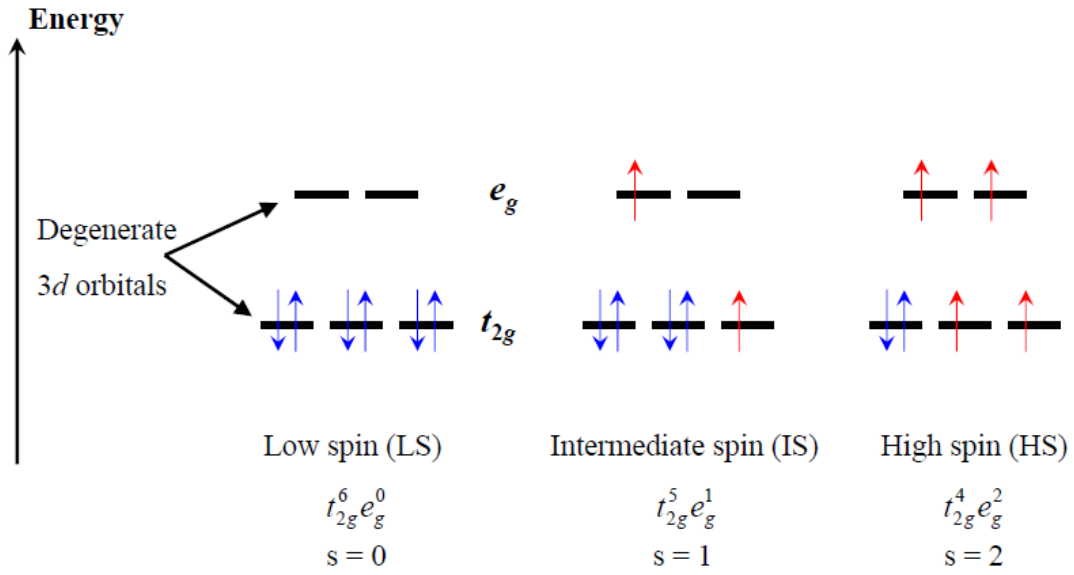

Figure S1. Three possible spin states of Co^{3+} in octahedral crystal field.

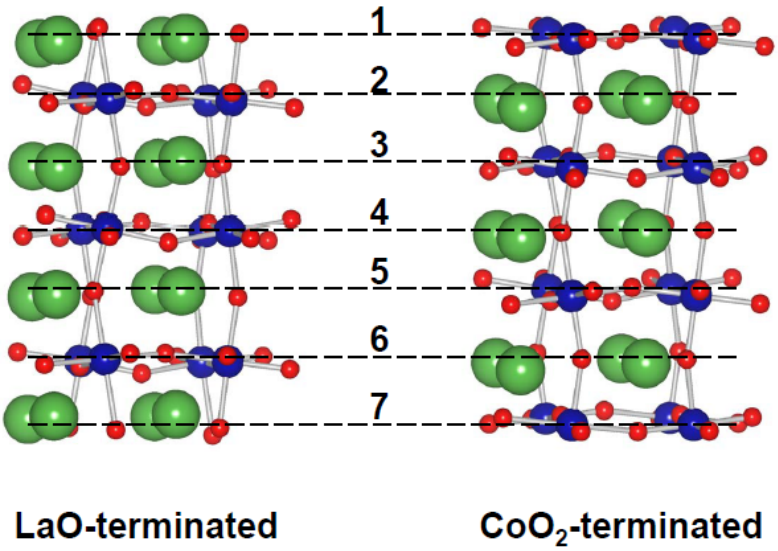

Figure S2. The layer numbered scheme of LaO-terminated and CoO_2-terminated (001) surfaces.

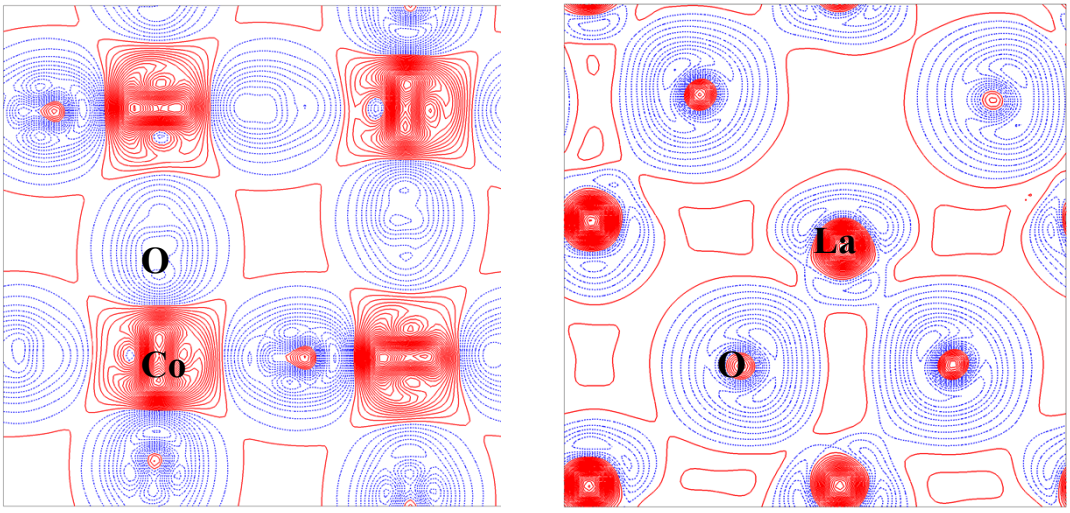

(*a*) (*b*)

Figure S3. The top-layer electron density difference maps of CoO_2-terminated (001) (*a*) and LaO-terminated (001) (*b*) surface slabs calculated with respect to the superposition of atomic densities. Solid (red) and dash (blue) lines represent deficiency and excess of the electron charge, respectively, with the increment of 0.003 e/Å^3.

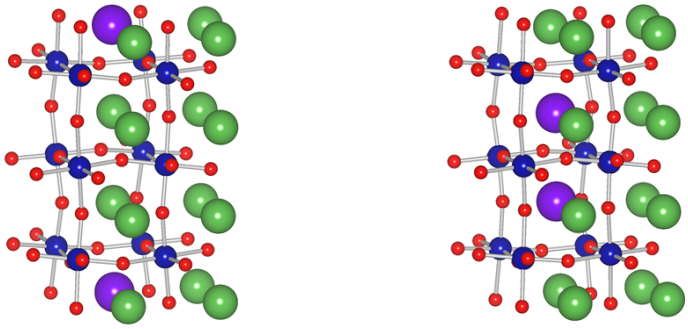

(*a*) 1,7-doping (*b*) 3,5-doping

(*c*) 2,6-doping (*d*) 4-doping

Figure S4. Side views of (*a*, *b*) LaO- and (*c*, *d*) CoO_2-terminated (001) surfaces with Sr-doping in different layers, respectively, doping level x_s = 25%.

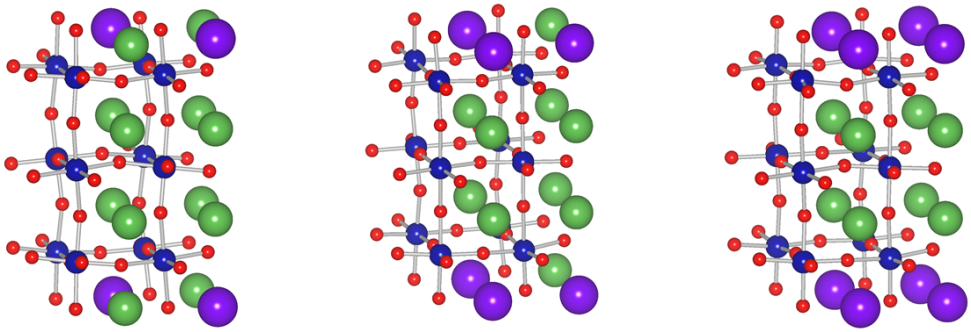

(*a*) x_s = 50% (*b*) x_s = 75% (*c*) x_s = 100%

(Ⅰ) LaO-terminated (001) surfaces

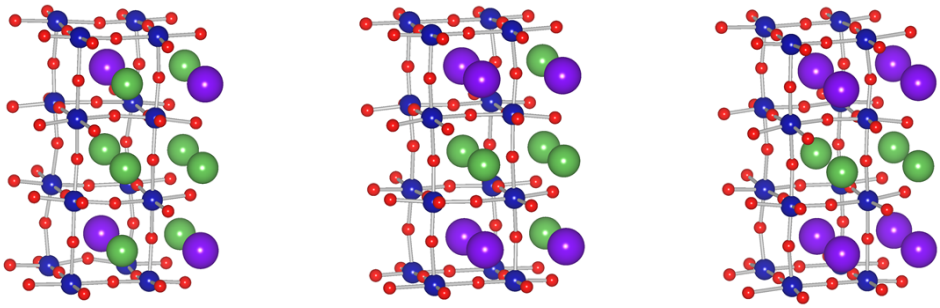

(*d*) x_s = 50% (*e*) x_s = 75% (*f*) x_s = 100%

(Ⅱ) CoO_2-terminated (001) surfaces

Figure S5. Side views of (*a-c*) LaO- and (*d-f*) CoO_2-terminated (001) surfaces with different Sr-doping levels (x_s = 50%, 75%, 100%) on the top layers, second layers of both sides, respectively.

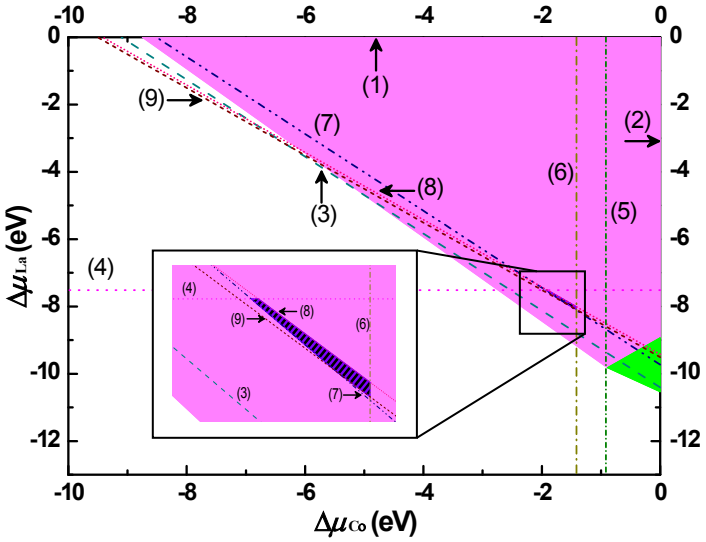

(*a*) x_s = 50%

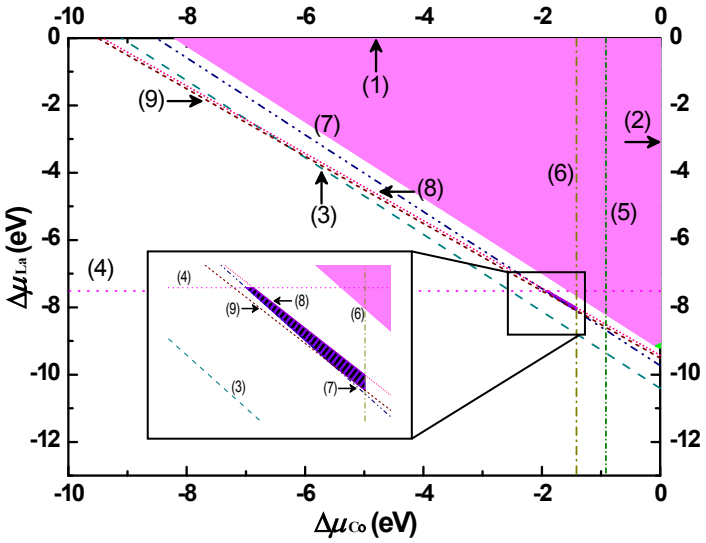

(*b*) x_s = 75%

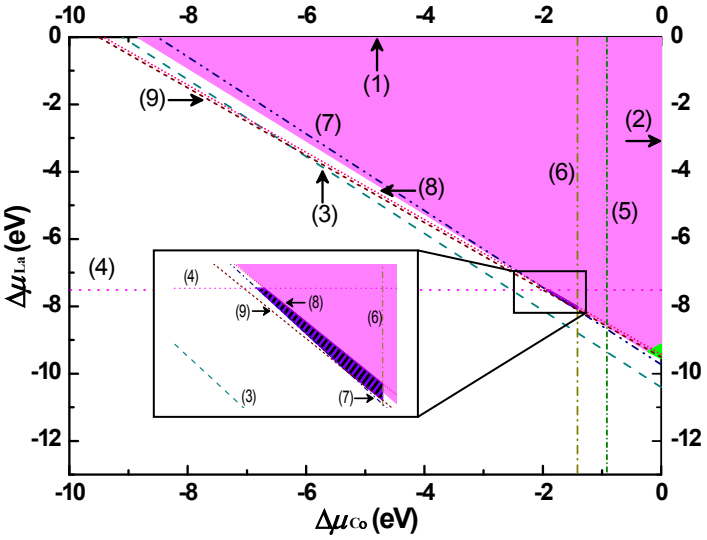

(*c*) x_s = 100%

LaO-(001) **CoO_2-(001)**

Figure S6. Phase diagrams for outermost-layer Sr-doped (001) surfaces with different terminations (x_s = 50%, 75%, 100%) of cubic $La_{0.875}Sr_{0.125}CoO_3$ system (T = 1100K, pO_2 = 0.2 atm). The numbers in parentheses point to lines, where phase separations of metals and their oxides from bulk $La_{0.875}Sr_{0.125}CoO_3$ begin to occur: (1) La, (2) Co, (3) Sr, (4) La_2O_3, (5) CoO, (6) Co_3O_4, (7) SrO, (8) $LaCoO_3$, (9) $SrCoO_3$. The hatched area among La_2O_3, Co_3O_4, $LaCoO_3$ and $SrCoO_3$ precipitation lines represents the stable region. Inset shows the magnified hatched area.

References:

(S1) A. Taylor and R. W. Floyd, *Acta Crystallographica*, 1950, **3**, 285.

(S2) J. J. Hanak and A. H. Daane, *Acta Crystallographica*, 1956, **9**, 559.

(S3) E. A. Sheldon and A. J. King, *Acta Crystallographica*, 1953, **6**, 100.

(S4) X. Liu and C. T. Prewitt, *Physics and Chemistry of Minerals*, 1990, **17**, 168.

(S5) S. Sasaki, K. Fujino and Y. Takeuchi, *Proceedings of the Japan Academy*, 1979, **55**, 43.

(S6) P. Aldebert and J. P. Traverse, *Materials Research Bulletin*, 1979, **14**, 303.

(S7) D. Taylor, *Transactions of the British Ceramic Society*, 1984, **83**, 5.

(S8) P. Bezdicka, A. Wattiaux, J. C. Grenier, M. Pouchard and P. Hagenmuller, *Zeitschrift fuer Anorganische und Allgemeine Chemie*, 1993, **619**, 7.

(S9) *NIST Computational Chemistry Comparison and Benchmark Database*, 14th ed. American Chemical Society: Washington DC, 2006.

(S10) G. Herzberg, *Molecular Spectra and Molecular Structure: Volume I - Spectra of Diatomic Molecules*, 2nd ed. Krieger Publishing Company: Malabar, FL, 1950.

(S11) A. D. John, *Lange's handbook of chemistry, 13th ed.* McGill-Hill Press, Knoxville, 1985.

(S12) S. N. Solov'ev, A. Y. Dupal and K. I. Shatalov, *Russian Journal of Physical Chemistry,* 2006, **80(12)**, 2049.

(S13) S. Stølen, F. Grønvold, H. Brinks, T. Atake and H. Mori, *J. Chem. Thermodynamics*, 1998, **30**, 365.

(S14) J. H. Cheng, A. Navrotsky, X. D. Zhou and H. U. Anderson, *J. Mater. Res.*, 2005, **20(1)**, 191.

(S15) H. Yokokawa, T. Kawada and M. Dokiya, *J. Am. Ceram. Soc.* 1989, **72,** 2104.

(S16) J. E. Saal, *Thermodynamic modeling of phase transformations and defects: from cobalt to doped cobaltate perovskites*. Dissertation, the Pennsylvania State University, Dec. 2010.